Geo-spatial Information Science 14(4):246-254
DOI 10.1007/s11806-011-0565-1

Volume 14, Issue 4
December 2011

Article ID: 1009-5020(2011)04-246-09

Document code: A

Remote Gully Erosion Mapping Using ASTER Data and Geomorphologic Analysis in the Main Ethiopian Rift

Moncef Bouaziz[1,2], Arief Wijaya[1,3], Richard Gloaguen[1]

1. Remote Sensing Group, Institut für Geologie, TU Bergakademie Freiberg, Bernhard-Von-Cotta Strasse 2, D-09596, Freiberg, Germany
2. Laboratoire 3E (AD-10-02), Ecole National d'Ingénieurs de Sfax, BP, 3038 Sfax, Tunisia
3. Faculty of Agricultural Technology, Gadjah Mada University, Sosio Yustisia 1, Bulaksumur, Yogyakarta 55281, Indonesia

Abstract The Main Ethiopian Rift (MER) is an area of extreme topography underlain by post-Miocene volcanic rocks, Jurassic limestone and a Precambrian basement. A prime concern is the rapid expansion of wide gullies that are impinging on agricultural land. We investigate the potential contribution of Advanced Space-borne Thermal Emission and Reflection Radiometer (ASTER) data and geomorphologic parameters to discern patterns and features of gully erosion in the MER. Maximum Likelihood Classification (MLC), Support Vector Machine (SVM), and Minimum Distance (MD) classifiers are used to extract different gully shapes and patterns. Several spatial textures based on Grey Level Co-occurrence Matrices (GLCMs) are then generated. Afterwards, the same classifiers are applied to the ASTER data combined with the spatial texture information. We used geomorphologic parameters extracted from SRTM and ASTER DEMs to describe the geomorphologic setting and the gullies' shapes. The classifications show accuracies varying between 67% and 89%. Maps derived from this quantitative analysis allow the monitoring and mapping of land degradation as a direct result of gully-widening. This study reveals the utility of combining ASTER data and spatial textural information in discerning areas affected by gully erosion.

Keywords remote sensing; gully erosion; texture; ASTER data

CLC number P237

Introduction

Gully erosion has a negative impact on soil features, crops, and water resources and is one of the main erosion processes in terms of resultant soil loss and sediment production across the world.[1-5] Several definitions are used to define the concepts and main characteristics of gullies. The Food and Agriculture Organisation (FAO) describes gullies as stream channels whose width and depth do not allow normal tillage.[6] Hudson (1985) defines gullies as steep- sided eroding water-courses that are subject to ephemeral flash floods during rainstorms. Gully erosion occurs at different rates and scales.[7] The causes, processes, prediction, and control of gully erosion have been studied in different environments and through several techniques.[1,8,9,10] A

► Received on April 25, 2011.

► Supported by the German Academic Exchange Service.

► Moncef Bouaziz is an environmental Engineer. The focus of his research is the monitoring of land degradation via remote sensing and GIS in arid and semiarid climate.

► E-mail: moncef. bouaziz@ gmail.com

study of 22 reservoir catchments in Spain clearly indicates that sediment yield increases when the frequency of gullies increases.[11] As well as being important in terms of soil degradation, gully erosion is also the main link between transfer runoff from uplands to valley bottoms.[3,12] Consequently, gully erosion is considered as one of the erosive processes that most contributes to shape the Earth's surface.[13]

The Main Ethiopian Rift (MER) is an area of extreme topography underlain by post-Miocene volcanic rocks, post-Triassic sediments and a Precambrian basement.[14] The MER is severely affected by wide gullies which are expanding into agricultural lands at an alarming rate.[15] The rapid increase in the number of areas affected by gully erosion in Ethiopia during recent decades has been variously attributed to deforestation, overgrazing, and climate change.[16] High temperature decreases the decomposition of organic matter and therefore can in turn, decrease soil stability, leading to gully formation.[17] Hitherto, the majority of land degradation studies related to gully erosion have been on a local scale and diagnostic with little or no focus on the mapping of gully shapes. Several gully erosion studies have been carried out in the Ethiopian Rift, including qualitative erosion mapping.[13,18,19] However, a standard method for gully erosion mapping is still lacking.[20] The main objective of these studies was to find out the type and severity of degraded soils associated with gullies according to different land-use types. The development of Geographic Information System (GIS), accurate Digital Elevation Model (DEM), and remote sensing techniques provide new possibilities to improve and optimize gully erosion mapping techniques.[1] Satellite scenes currently cover almost the whole Earth, providing interesting capacities to investigate gullies wherever required. Giordano and Marchisio (1991) revealed that gullies affect areas wide enough to be covered by the resolution of satellite images.[21] Therefore, multispectral remote sensing techniques are becoming increasingly relied upon to map the extension of gully erosion phenomena[22-24] and to generate maps showing the erosional activity of gully walls from mapped vegetation cover.[24]

A spatial mapping and assessment of the gullies in the MER region is required to fully describe and understand this phenomenon. The main objective of this current work was to map areas affected by gully erosion and to develop a methodology based on remote sensing data to provide regional-scale, gully erosion-intensity maps. Algorithms for image classification, spectral properties, texture feature information, and geomorphologic analysis were used for this purpose. Consequently, we describe the potential contribution of Advanced Space-borne Thermal Emission and Reflection Radiometer (ASTER) data and geomorphologic parameters to discern gully erosion in the MER.

1 Study areas

Two different study areas within the MER were selected for this research. Test sites *A* and *B* were selected as representatives of typical catchments where gully erosion is encountered on a large scale. In addition, they highlight two different types of gullies (discontinuous and continuous). The visual interpretation of the RGB ASTER image shows much spreading of discontinuous gullies in region *A*, whereas the continuous gullies are widely present in region *B*.

The test sites are located in the central part of the MER in the northeast of Africa between longitude 38° and 39° and latitude 8° and 9° North (Fig.1). The average annual rainfall is approximately 720 mm. The main rainy season extends from late May to September. Region *A* is dominated by pastureland, used by the people of the ALEMA TENA village for cattle grazing. The presence of the village, with a few hundred families has led to a landscape in sharp contrast to that in region *B*. Region *B* is dominated by cropland, savannah, and rangeland.

Both study areas are situated in a sub-humid tropical environment but exhibit differing geomorphology. Area *B* is characterized by chains of hills and steep slopes (average $>$ 25°) with an average elevation of 1765 m asl. Area *A* has a more undulating topography with gentle slopes and an average elevation of 1643 m asl. Slopes in both areas are often highly dissected by *V*-shaped and concave valleys.

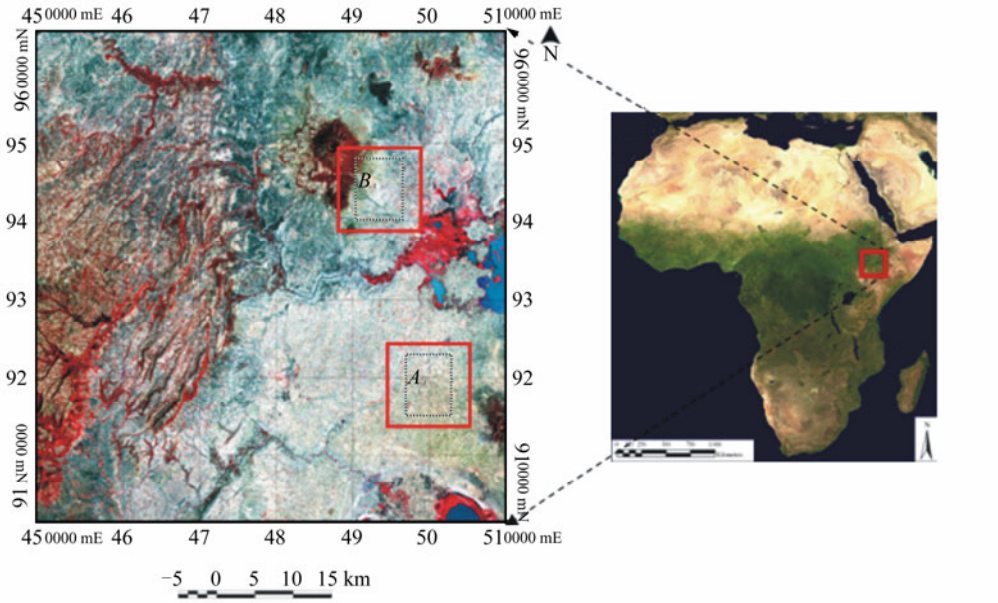

(a) Subset from ASTER image acquired in October 2006 (b) Composed MODIS image of Africa from 2005

Fig. 1 Location of study areas in the MER

2 Data and methodology

Different methods have been proposed for the extraction and classification of gully erosion.[8,9] A methodological framework in the context of remote sensing and GIS techniques was considered to carry out this study. Algorithms for image classification as Maximum Likelihood Classification (MLC), Support Vector Machine (SVM), and Minimum Distance (MD) were used to extract the various gully shapes and patterns.

(1) Support vector machine

The SVM is a type of universal learning machine, used for pattern recognition and originally designed to solve binary classification problems.[25] The SVM classification requires a proper selection of kernel function to establish accurate hyperplanes that minimize misclassification error.[25] The Radial Basis Function (RBF) kernel was selected for the classification and works well for general image classification cases.[26]

The mathematical representation of the RBF kernel (K) is:

$$K(x_i, x_j) = \exp(-\frac{\|x_i - x_j\|^2}{2\sigma^2}) \quad (1)$$

Where data separability are represented by $\{x_i, x_j\}$ and σ is the width of the radial basis function.

(2)Maximum likelihood classification

Maximum likelihood classification is the most widely adopted parametric classification algorithm.[27-29] MLC algorithm is based on probability distributions and decision rules which assume the date values to be a set of multivariate normal distributions.[30] The algorithm classification assigns a particular class to each pixel based on the shortest modified distance of the pixel from the class mean. It also considers shape, size and orientation of the training samples

(3)Minimum distance classification

Supervised MD classification was also applied in this study. It is a simple classification algorithm which uses the mean vectors of each endmember and calculates the Euclidean distance from each unknown pixel to the mean vector for each class.[31] All pixels are classified to the nearest class unless a standard deviation or distance threshold is specified, in which case some pixels may be unclassified if they do not meet the selected criteria. The MD algorithm is fast and one of the more commonly used algorithms because of its mathematic simplicity.

Classification accuracies were assessed using confusion matrices. Sample data of gully and non-gully erosions were initially selected from the satellite image and confirmed with the information collected during fieldwork, which was then used to run the classification.

ASTER image Level 1B data, acquired in October 2006, is used for the purpose of this work. The image

has a spatial resolution of 15 m in three Visible and Near Infrared (VNIR) bands, 30 m in the nine Short Wave Infrared (SWIR) bands and 90 m in the 5 bands of the Thermal Infrared (TIR). Atmospheric correction was conducted on this image using ENVI FLAASH to produce surface reflectance from a multispectral radiance ASTER scene and compensate for atmospheric effects.

In addition, DEM was generated from the ASTER stereo image using the 3N (nadir) and 3B (backward) bands of the ASTER data. Therefore, 175 tie points were collected to connect the 3N and 3B channels using the OrthoEngine toolbox in the PCI Geomatica environment. These images have a size of 4200 × 4100 pixels with a spatial resolution of 15 m. The generated DEM employed Ground Control Points (GCPs) from a 1:25000 scale topographic map and Shuttle Radar Topographic Mission (SRTM) data.

Furthermore, we selected a number of predisposing factors to accurately identify soils affected by gullies. Slope, elevation and drainage networks are considered as important factors in susceptibility studies of soil denudation.[32-34] These factors were used to validate the MLC, SVM and MD supervised classification results. Layers representing the appointed factors were overlapped on the classification results and used to validate the classification through visual interpretation.

The extraction of the drainage network was generated automatically based on the deterministic 8 (D8) model and by direct digitalization of the ASTER image.[35,36] The D8 methodology considers eight flow directions, four horizontal and vertical, and four diagonal. The model determines the steepest down slope between a cell and a neighbouring cell, taking into consideration the elevation of the closest cells and the distance between the centres of cells.

Maps derived from such analyses allowed the identification and description of forms and patterns of gullies that were encountered in the study areas on a catchment scale. The general methodological procedure is presented in the Fig.2.

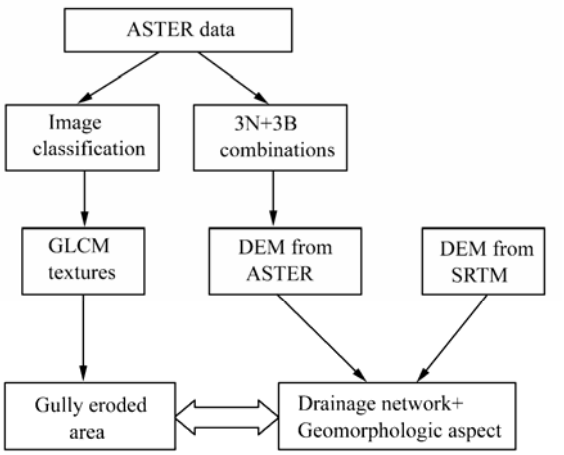

Fig. 2 Diagram of mapping the gully erosion using remote sensing and geomorphology analysis

2.1 Training sample preparation

Selection of the training samples is an important stage in supervised satellite image classification procedures. Collected sample datasets are fed into the classification algorithms to discriminate the gully erosion with other classes. In land degradation mapping the definition of training features is a crucial step as an incorrect definition/selection of training areas may compromise the outcome of classification.[37] Training areas were selected based on the knowledge and information available from the region. This was acquired during fieldwork and then combined with geomorphologic aspects collected from the SRTM and ASTER DEM data. Furthermore, shaded relief, aspect angle, and drainage network from the DEM were generated and used as additional spectral data information to discriminate the pattern of gullies from the non-gullies.

For better discrimination in selecting training samples from ASTER image classes, we used the results of unsupervised algorithms to help define the training features. The *k*-means clustering method was selected to obtain probable clusters. In addition, visual interpretation from RGB composition and reference maps were considered for a better definition of the training sets. According to Lu and Weng (2005), such a procedure is a hierarchical development to obtain the best possible result from the classification approach.[38] To conduct SVM, MLC and MD supervised classifiers, two classes were defined: gullies (i.e. where we find gullies with river beds and gullies without river beds) and non-gullies (i.e. other land use classes, such as bare soil, irrigation area, urban, and savannah). We adopt an approach similar to that applied by Liberti *et al*. (2009) to discern badland areas in southern Italy, which has similar climate conditions as the study areas.[17]

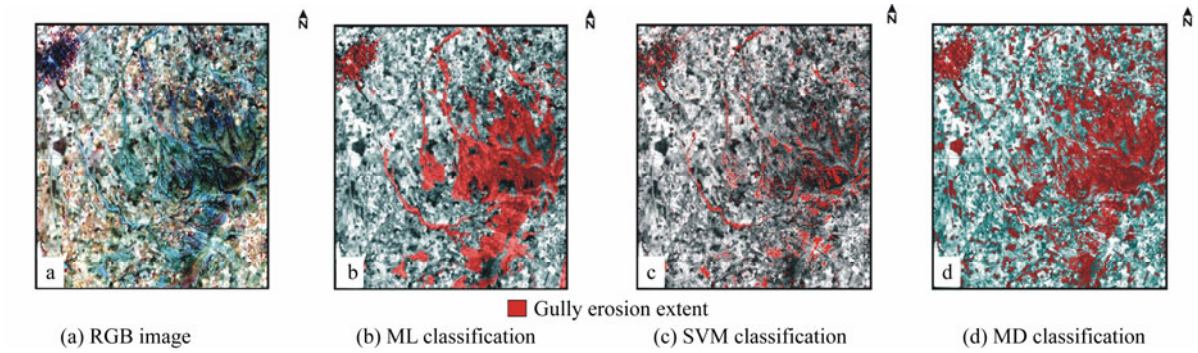

Fig. 3 Gully area extent maps in the region *A*

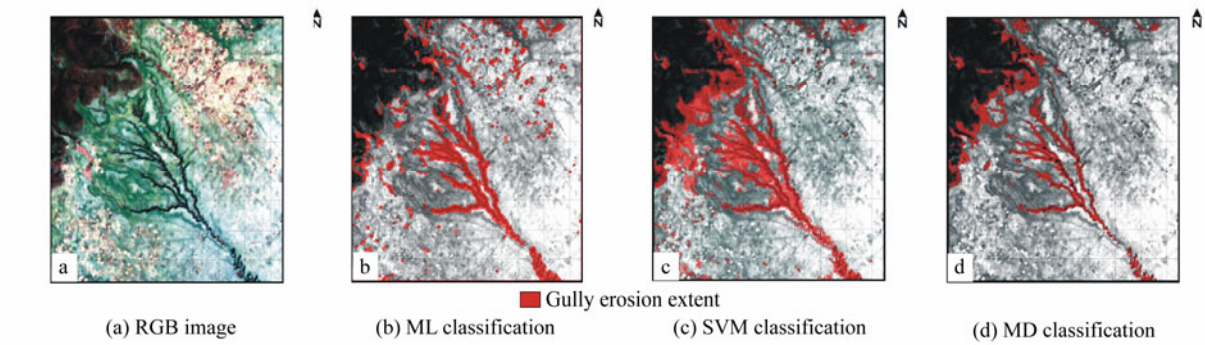

Fig. 4 Gully area extent maps in the region *B*

2.2 Spatial texture information approach

According to Irland *et al*. (1939), gully classification requires a description of forms and patterns.[10] Hilsky (1973) suggested that classification of gullies should be based on gully form (in plan), gully side morphology, and the shape of the transverse and longitudinal profiles.[39]

In this study, we analyzed the variability of spatial texture information for land degradation by gullies. Measures of texture based on the Grey Level Co-occurrence Matrix (GLCM) were used to extract spatial information from the image.[25] This technique can be presented as a tabulation of how different combinations of pixel brightness values (grey level) occur in an image. [27] Several texture layers results from this technique, namely mean, variance, homogeneity, contrast, dissimilarity, entropy, second moment, and correlation were computed from each pixel and its horizontal neighbours. We experimented with these textures to find out the textures that were showing additional spectral information for the classification. We found that mean, variance, and contrast textures are useful for distinguishing between gullies and non-gullies. These three texture features were combined with VNIR and SWIR bands and used to discern the patterns of gully erosion.

To remove spurious pixels within a large single class, we used the majority analysis during post-classification processing. Several attempts to find a suitable kernel size were carried out, with the 3×3 kernel producing the most favourable results.

3 Results and discussion

3.1 Spectral properties of gullies

Spectral analysis was performed in this study to describe spectral behaviours of the gullies. Reflectance values were extracted for the predefined classes in order to demonstrate the spectral characteristics of the gullies. For this purpose, four types of gully and non-gully classes are chosen from the two selected test sites. Approximately 200 pixels were chosen to represent each class (i.e. continuous gullies, discontinuous gullies, bare soil and urban region). Discontinuous gullies in our study represent the initial stages of development, typically when the more rapid rate of gully expansion occurs.[40] These gullies develop through side-wall erosion and collapse, soil pipes and collapsed cavities then become continuous gullies as they connect to other gullies.[22] The average of the spectral response of each training

shows a standard deviation that does not exceed 3% for all spectral responses (Fig. 5). Reflectance values reveal mostly non-stressed information for gully-affected soils. The spectral profiles of the urban area and gully erosion with the depth streaming bed are stressed and intermixed. This is in agreement with the findings of the classification algorithms, where misclassified gullies in the test site *A* are mostly because of the high similarity of the reflectance with the urban areas.

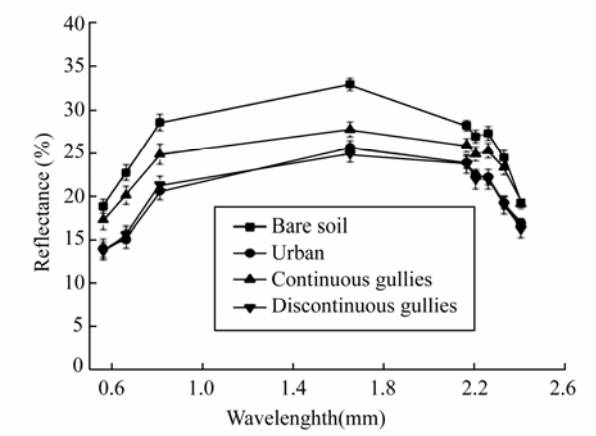

Fig. 5 Average of spectral signatures of different classes from ASTER

3.2 Methodology

3.2.1 *Gully erosion mapping*

The geomorphologic setting shows that 15% and 9% of the gullies in the test sites *A* and *B* are affected by permanent gullies. The classification results were assessed using confusion matrices. The accuracies were 87% and 89% for the test sites *A* and *B*, respectively (Figs. 7 and 8). This is explained by the high development of discontinuous gullies in area *A*, where the floor has a shallower gradient than the surrounding area and is composed of newly deposited material layer over an undisturbed alluvium.[41] Therefore, to correctly distinguish gully spreading in test site *A* is problematic. This highlights the necessity of additional information (especially ground truth data or very high resolution images), which can enhance the accuracy for such a study. Fig. 6 shows that GLCM texture features reduced misclassified pixels in the north-western part of the study area mostly affected by discontinuous gullies. The enhanced contrast effects from the texture features may explain this

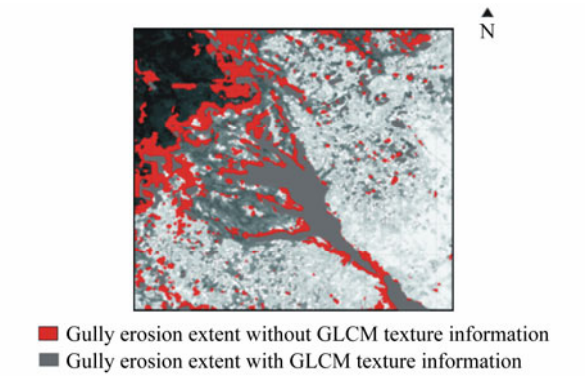

Fig. 6 Comparison the MLC results using spectral data and GLCM texture information

accuracy improvement.

In the eastern part of area *A* and the western part of area *B*, gully channels are narrow and have V-shaped forms coupled with steep slopes. Gully erosion occurred predominantly in areas of pasture and bare soil. Gully shapes are more prominent from June to September during the rainy season. During this time, under heavy rain, many gullies are reactivated and in addition to vertical dissection, may frequently undergo headwards retreat and lateral spreading.[34] The test site *A* displays higher occurrence of discontinuous gullies, which result in the development of badlands. Here, the forms and patterns of badlands are clear and characterized by short and narrow channels. The majority of the non-identified gullies are located in the upper reaches of channels where gullies are thin and difficult to detect using solely the spectral reflectance data. The classification accuracies vary between 67 %, 72 %, and 68 % without incorporation of the GLCM texture features and 77 %, 87 %, and 73% combined with the GLCM textures, resulting from the MLC, SVM, and MD classifiers, respectively (Figs.7 and 8).

SVM classification performs better than other methods to identify gullies in test site *A*, which is not the case for area *B*, where MLC outperforms other classifiers (Fig. 8). We initially tried to find the best possible algorithm suitable for gully erosion classification, but finding out how one classifier performs better than another is beyond the scope of our study. References do not mainly link classifier performance to the substance of these algorithms. Nevertheless, the potential exists that such models may be linked to spatially-explicit land use change models.[42]

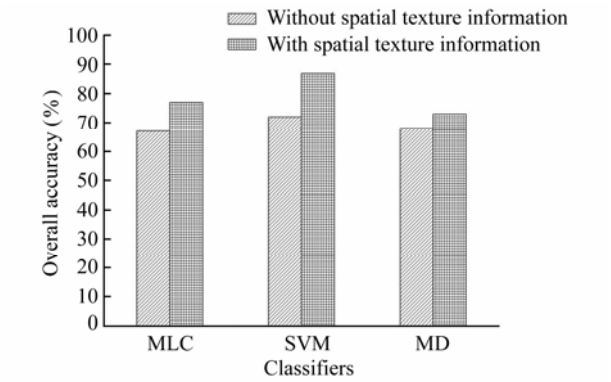

Fig. 7 Classification accuracy for area *A*

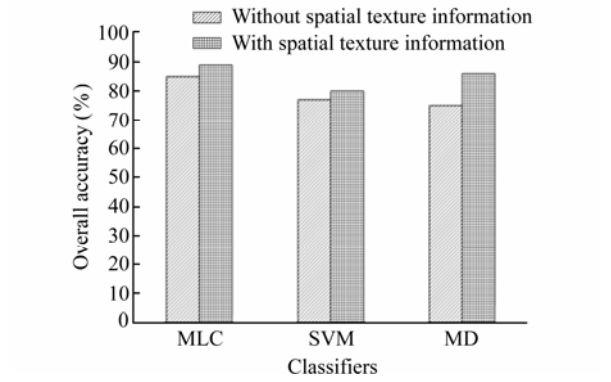

Fig. 8 Classification accuracy for area *B*

3.2.2 *Gully controlling factors from remote sensing data*

Because of the low spatial resolution of SRTM data (90 m), ASTER DEM (15 m) data provides better results to identify affected soils by gullies over small scales. We found that the ASTER DEM data highlighted more accurate shapes and patterns for recognized gullies. According to the classification results, the drainage network extracted from ASTER DEM shows high-density feeders within the areas that are highly affected by gullies.

The GLCM texture information greatly improved the classification results, as shown in Figs. 7 and 8, which reveal an improvement within all the classifications. The combination of ASTER data and GLCM texture features are more sensitive to identify discontinuous gullies, showing a 6% increase in the classification accuracy for three classifiers. When combining GLCM texture features with the spectral data, the accuracy improvement of test area *A* is higher than that of test area *B*.

Geomorphologic parameters (shaded relief, aspect, and slopes) and acquired information from fieldwork were used to select ground truth to assess the classification accuracy using confusion matrices. Furthermore, classification results were overlaid with the geomorphologic parameters in order to localize the over-and-under estimation of gullies of each classifier. The extent of the gully class was compared with the edge from the shaded relief and aspect maps. Visual interpretation in this case was successful and highlighted the location of erroneous and misclassified areas affected by gully erosion.

The identification of gully erosion could be improved by combining the classification results (gullies and non-gullies) with several controlling factors such as land use, DEM, vegetation cover, rainfall, and lithology. The present study considers relatively small areas; a larger study area should consider these additional controlling factors.

The above methodology could be applied to images acquired from several satellites. Higher spatial resolution (e.g. IKONOS, QuickBird, etc) may certainly reduce the spectral mixing problem. Nevertheless, limited spatial cover, low spectral resolution, and high acquisition costs characterize very high-resolution data and are a limiting factor for gully erosion mapping. [20] The proposed approach to discern gully erosion at the catchment scale by combining digital DEM from both ASTER and SRTM images and GIS was effective for the discrimination of gullies. A goal for future work will be to establish the various controlling factors that must be considered when predicting future gully erosion within a regional scale.

4 Conclusion

This work highlights the utility of ASTER data, spatial textural information and geomorphologic parameters in discerning areas affected by gully erosion in the region. The results of this study showed that textural layers estimated from a GLCM significantly improved spectral data classification of the ASTER image. MLC, SVM, and MD classifications were conducted to discern gullies in two different test sites. The confusion matrix resulted in two different but encouraging accuracy results (between 67 % and 89 %). The urban surface misclassification and highly developed discontinuous gullies in test area *A* could explain the lower accuracy as compared with test area *B*.

Visual interpretation of the DEM extracted from an ASTER image using the 3N and 3B bands led to a greater detail in the patterns of gully erosion. In this case, a higher spatial resolution of the ASTER image was achieved compared with the DEM derived from SRTM data. Geomorphologic parameters from the ASTER image play an important role in discriminating the features and patterns of gullies. These geomorphologic parameters were useful for validating the results from both the algorithms and textural features used to discern areas affected by gullies. The drainage network map, for example, shows a high density of feeders located in the areas identified as suffering from gully erosion.

Our results suggest that the semi-automatic identification of gully erosion using ASTER optical data is an effective approach towards a better understanding of the occurrences of this form of land degradation. This new approach can now be transferred to other areas for further evaluation.

Acknowledgements

The authors gratefully acknowledge the DAAD (German Academic Exchange Service) for honoring the first author with the scholarly award to pursue his PhD at the Technische Universität Bergakademie Freiberg, Germany

References

[1] Martínez-Casasnovas J A (2003) A spatial information technology approach for the mapping and quantification of gully erosion [J]. *Catena*, 50: 293-308

[2] Valentin C, Rajot J L, Mitja D (2004) Responses of soil crusting, runoff and erosion to fallowing in the sub-humid and semi-arid regions of West Africa [J]. *Agriculture, Ecosystems & Environment*, 104(2): 287-302

[3] Poesen J, Valentin C (2003) Preface of special issue of Catena: gully erosion and global change [J]. *Catena*, 50: (2-4): 87-89

[4] Singh G, Babu P, Narain L S, et al. (1992) Soil erosion rates in India [J]. *J. Soil Water Conserv*., 47 (1): 97-99

[5] Ygarden L (2003) Rill and gully development during and extreme winter runoff event in Norway [J]. *Catena*, 50 (2-4): 217-242

[6] Food and Agriculture Organization (FAO) (1965) Soil erosion by water. Some measures for its control on cultivated lands. Rome [R]. FAO Agriculture Paper 81

[7] Hudson N W (1985) Soil conservation. London: Batsford. Conservation practices and runoff water disposal on steep lands. Moldenhauer W C, Hudson N W (Eds). Conservation farming on steep lands [M]. Ankeny: SWCS

[8] Boardman J, Parsons A J, Holland R, et al. (2003) Development of badlands and gullies in the Sneeuberg, Great Karoo, South Africa [J]. *Catena*, 50: 165-184

[9] Shibru D, Wolfgang R, Peter S (2003) Assessment of gully erosion in eastern Ethiopia using photogrammetric techniques [J]. *Catena*, 50: 273-291

[10] Ireland H A, Sharpe C F, Eargle D H (1939) Peinciples of gully erosion in the piedmont of south Carolina [R]. Washington DC: US Department of Agriculture, Technival Bulletin 633

[11] Verstraeten G, Poesen J, de Vente J, et al. (2003) Sediment yield variability in Spain: a quantitative and semiqualitative analysis using reservoir sedimentation rates [J]. *Geomorphology*, 50(4): 327-348

[12] Poesen J, Vandekerckhove L, Nachtegaele J, et al. (2002) Gully erosion in dryland environments [M]// Bull M J, Kirkby M J (Eds). Dryland Rivers: Hydrology and Geomorphology of Semi-arid Channels. Chichester, UK: John Wiley and Sons

[13] Billi P, Dramis F (2003) Geomorphological investigation on gully erosion in the the Rift valley and the northern highlands of Ethiopia [J]. *Catena*, 50(2-4): 353-368

[14] Yusuke K (2007) Regional scaled mapping of gully erosion sensitivity in Western Kenya [J]. *African Journal of Environmental Science and Technology*, 1(3): 49-52

[15] Bouaziz M, Leidig M, Knoche M, et al. (2009) Contribution of remote sensing and GIS to the qualitative assessment of eroded surfaces in the main Ethiopian rift [J]. *Publikationen der Deutschen Gesellschaft für Photogrammetrie, Fernerkundung und Geoinformation*: 175- 182

[16] Sagri M (1998) Land resources inventory, environmental changes analysis and their application to agriculture in the Lakes region Ethiopia [R]. European Commission Contract TS3-CT92-0076 Fina report

[17] Liberti M, Simoniello T, Carone M T, et al. (2009) Mapping badland areas using LANDSAT TM/ETM satellite imagery and morphological data [J]. *Journal of Geomorphology*, 106: 333-343

[18] Daba S (2003) An investigation of the physical and socioeconomic determinants of soil erosion in the Hararghe

highlands, eastern Ethiopia [J]. *Land Degrad. Develop*., 14(1): 69-81

[19] Nyssen J, Poesen J, Moeyersons J, et al. (2002) Impact of road building on gully erosion risk: A case study from the northern Ethiopian highlands [J]. *Earth Surf. Process. Landforms*, 27(12): 1267-1283

[20] Vrieling A, de Jong S M, Sterk G, et al. (2008) Timing of erosion and satellite data: A multi-resolution approach to soil erosion risk mapping [J]. *International Journal of Applied Earth Observation and Geoinformation*, 10(3): 267-281

[21] Giordano A, Marchisio C (1991) Analysis and correlation of the existing soil erosion maps in the Mediterranean basin [J]. *Quaderni di Scienza del Suolo*, 3: 97-132

[22] Bocco G (1990) Gully erosion analysis using remote sensing and GIS [D]. Amsterdam: University of Amsterdam

[23] Sole` Ll, Clotet N, Gallart F, et al (1986) Ana´lisis de las posibilidades de las ima´genes TM en la deteccio´n de a´reas degradadas en sectores montan˜osos [M]//Clotet N, Sole` L l (Eds). Coumunicaciones Cientı´ficas de la I Reunio´n Cientı´fica del Grupo de Trabajo de Teledeteccio´n. Jaume Almera, Barcelona: Institut d'Investigacions Geolo`giques

[24] Martı´nez-Casasnovas J A, Poch R M (1998) Estado de conservacio´n de los suelos de la cuenca del embalse Joaquı´n Costa [J]. *Limnetica*, 14: 83-91

[25] Wijaya A, Marpu P R, Gloaguen R (2008) Geostatistics texture classification of tropical rainforests in Indonesia [M]//Stein S, Bijker (Eds). Quality in Spatial Data Mining. CRC Book Series

[26] Hall-Bayer M (2000) GLCM texture: A tutorial [R]. National Council on Geographic Information and Analysis Remote Sensing Core Curriculum

[27] Jensen J R (2005) Thematic map accuracy assessment. Introductory digital image processing – A remote sensing Perspective [M]//Keith C Clarke (Eds). Prentice Hall Series in Geographic Information Science

[28] Bailly J S, Arnaud M, Puech C (2007) Boosting: a classification method for remote sensing [J]. *International Journal of Applied Earth Observation and Geoinformation*, 7: 232-247

[29] Liu X H, Skidmore A K, Oosten H V (2002) Integration of classification methods for improvement of land cover map accuracy [J]. *ISPRS Journal of Photogrammetry & Remote Sensing*, 56: 257-268

[30] Manadhar R, Odeh I O, Ancev T (2009) Imroving the accuracy of land use and land cover classification of landsat data using post classification Enhancement [J]. *Remote Sensing*, 1: 330-344

[31] Richards J A, Jia X (1999) Remote sensing digital image analysis (3rd Ed). [M]. Berlin: Springer-Verlag

[32] Carrara A, Cardinali M, Detti R, et al. (1991) GIS techniques and statistical models in evaluating landslide hazard [J]. *Earth Surf Proc Land*, 16: 427-445

[33] Maharaj R (1993) Landslide processes and landslide susceptibility analysis from an upland watershed: A case study from St Andrew, Jamaica, West Indies [J]. *Eng Geol*, 34: 53-79

[34] Guzzetti F, Carrara A, Cardinali M, et al. (1999) Landslide hazard evaluation: A review of current techniques and their application in a multi-scale study, Central Italy [J]. *Geomorphology*, 31: 181-216

[35] O'Callaghan J, Mark D (1984) The extraction of drainage networks from digital elevation data [J]. *Computer Vision, Graphics and Image Processing*, 28: 323-344

[36] Tarboton D G. (1997) A new method for the determination of flow directions and upslope areas in grid digital elevation models [J]. *Water Resour. Res*., 33(2): 309-319

[37] Foody G M (2002) Status of land covers classification accuracy assessment [J]. *Remote Sensing of Environment*, 80: 185-201

[38] Lu D, Weng Q (2005) Urban classification using full spectral information of LANDSAT ETM+ Imagery in Marion County, Indiana [J]. *Photogrammetric Engineering and Remote Sensing*, 71: 1275-1284

[39] Hilsky H (1973) Erosion en Carcavas. Havana: Academia de Cieencias de Cuba (special publication) [J]. *I. De Geologia*

[40] Sidorchuk A (1999) Dynamic and static models of gully erosion [J]. *Catena*, 37(3-4): 401-414

[41] Leopold L B, Wolman G M, Miller J P (1964) Fluvial processes in geomorphology [M]. New York: W.H. Freeman and Company

[42] Veldkamp A, Lambin E F (2001) Predicting land-use change [J]. *Agriculture Ecosystems & Environment*, 85 (1-3): 1-6